Cryosurgery: Analysis and Experimentation of Cryoprobes in Phase Changing Media

Avraham Shitzer
Department of Mechanical Engineering,
Technion, Israel Institute of Technology,
Haifa 32000, Israel
e-mail: mersasa@tx.technion.ac.il

This article presents a retrospective of work performed at the Technion, Israel Institute of Technology, over the last 3-odd decades. Results of analytical and numerical studies are presented briefly as well as in vitro and in vivo experimental data and their comparison to the derived results. Studies include the analysis of both the direct (Stefan) and the inverse-Stefan phase-change heat transfer problems in a tissue-simulating medium (gel) by the application of both surface and insertion cryoprobes. The effects of blood perfusion and metabolic heat generation rates on the advancement of the freezing front are discussed. The simultaneous operation of needle cryoprobes in a number of different configurations and the effects of a thermally significant blood vessel in the vicinity of the cryoprobe are also presented. Typical results demonstrate that metabolic rate in the yet nonfrozen tissue, will have only minor effects on the advancement of the frozen front. Capillary blood perfusion, on the other hand, does affect the course of change of the temperature distribution, hindering, as it is increased, the advancement of the frozen front. The volumes enclosed by the "lethal" isotherm (assumed as −40°C), achieve most of their final size in the first few minutes of operation, thus obviating the need for prolonged applications. Volumes occupied by this lethal isotherm were shown to be rather small. Thus, after 10 min of operation, these volumes will occupy only about 6% (single probe), 6–11% (two probes, varying distances apart), and 6–15% (three probes, different placement configurations), relative to the total frozen volume. For cryosurgery to become the treatment-of-choice, much more work will be required to cover the following issues: (1) A clear cut understanding and definition of the tissue-specific thermal conditions that are required to ensure the complete destruction of a tissue undergoing a controlled cryosurgical process. (2) Comprehensive analyses of the complete freeze/thaw cycle(s) and it effects on the final outcome. (3) Improved technical means to control the temperature variations of the cryoprobe to achieve the desired thermal conditions required for tissue destruction. (4) Improvement in the pretreatment design process to include optimal placement schemes of multiprobes and their separate and specific operation. (5) Understanding the effects of thermally significant blood vessels, and other related thermal perturbations, which are situated adjacent to, or even within, the tissue volume to be treated. [DOI: 10.1115/1.4002302]

Keywords: inverse problem, lethal temperature, cooling rate, frozen volume

1 Introduction

Cryosurgery is a medical technique involving the application of extremely low (cryogenic) temperatures with an aim to destroy abnormal or diseased tissues by freezing [1]. Applications include the treatment of a variety of benign and malignant skin conditions and diseases of internal organs (e.g., prostate). Cryosurgery was in use as early as in the middle 19th century when James Arnott, an English physician, used salt-ice mixtures to treat malignant tumors [2]. The so-called "modern era" of cryosurgery was evidently initiated in 1961, when Irving Cooper, an American neurosurgeon, developed a liquid nitrogen-based cryosurgical system [3]. In this system the cryofluid was used in a heat conducting metal tube, the closed end of its tip was brought into contact with the treated tissue. This design still forms the basis for a variety of instruments used in this field to date.

The destruction of biological tissues by the application of freezing-thawing cycles may be achieved by either, or a combination of the following processes: immediate and delayed. The immediate process involves direct destruction of cells and is dominated by the various modes of extra- and intracellular ice formation during the freezing stage. The delayed, post-application destruction mechanisms are due to damages resulting from the destruction of blood vessels and/or an invoked immune system response.

The key advantages of the cryosurgical procedure are as follows: (a) it is minimally invasive, (b) the application is localized (in situ), (c) it causes minimal trauma to the patient, (d) it involves minimal loss of blood, (e) it possesses anesthetic capabilities due to the subfreezing temperatures involved, (f) its application duration is relatively short, (g) it is cycleable and repeatable (h), it requires minimal hospitalization, or it might even be applied ambulatorily, (i) it incurs relatively low costs, and (j) in certain cases, it may invoke a delayed immune system response to remove the undesired, recently frozen tissue.

In spite of these apparent advantages, the cryosurgical technique is still finding only limited applications, mainly in urology [4] and in dermatology [5]. The reason for this lack of wider applicability stems mainly from the following reasons: (a) the uncertainty in the final outcome of the procedure since the identical physical mechanism, namely, *in vivo* tissue freezing, is also used to achieve quite the opposite outcome—tissue preservation, compare Ref. [6], (b) the inability to ensure complete freezing of the entire target volume, in a short application due usually to its irregular shape, (c) possible undesired excessive damage to sur-

Manuscript received January 7, 2010; final manuscript received February 3, 2010; published online September 27, 2010. Assoc. Editor: Andrey Kuznetsov.

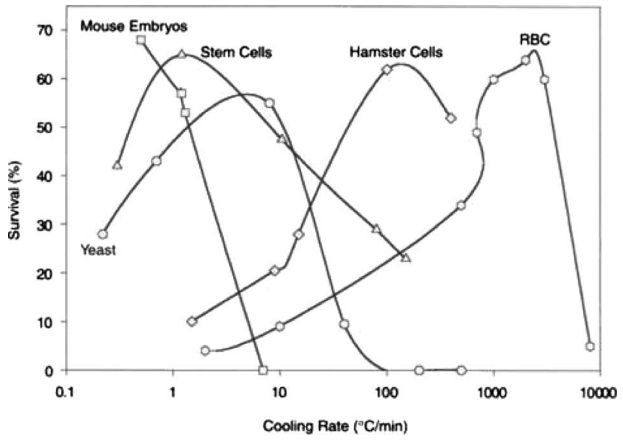

Fig. 1 Cell survival versus cooling rate applied [11]. (This figure originally appeared in an article by J.K. Critser and L.E. Mobraaten in ILAR Journal 41(1). It is reprinted with permission from the ILAR Journal, Institute for Laboratory Animal Research, The National Academies, Washington DC (www.nationalacademies.org/ilar)).

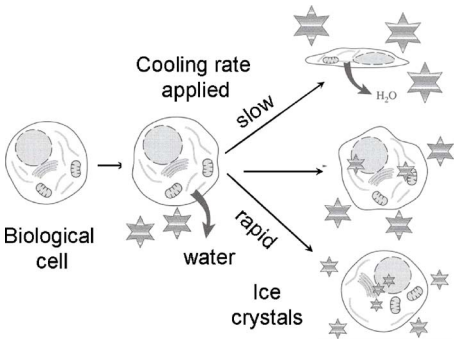

Fig. 2 Effects of cooling rates applied to biological cells on intra- and extracellular water freezing

rounding healthy tissues and adjacent major blood vessels, (d) difficulties in controlling the extent of the frozen volumes, (e) difficulties in monitoring the precise temperature distributions in the tissue during each freeze-thaw cycle, and (f) susceptibility to thermal perturbations by adjacent thermally significant blood vessel(s).

The simultaneous application of multiprobes, coupled with the use of modern imaging techniques, e.g., ultrasound, computerized tomography (CT) and magnetic resonance imaging (MRI), have alleviated some of these hindrances to a certain extent and have extended the use of cryosurgery in the treatment of prostate and liver cancer [1,4]. These imaging techniques, however, are still incapable of acquiring detailed temperature distribution data inside the frozen volume. Ultrasound, which is the most commonly applied imaging technique in cryosurgery, has its own limitations. Among these is the opaqueness of the frozen phase to sound waves due to ice formation. Thus, obtaining detailed, temporal, three-dimensional temperature distribution data inside the freezing tissue behind the frozen front by ultrasound is not possible. Currently, even the more expensive and complex CT or MRI imaging techniques, are incapable of providing temperature distribution details inside the frozen volume.

An effective cryosurgical treatment, particularly of malignant tissues, requires that optimal tissue destruction conditions be achieved throughout the entire volume of the tumor, including a predetermined margin for certainty. It is well known that different types of tissue cells exhibit different sensitivities to freezing but, as a general rule, the lower the temperature achieved, the higher the probability of destruction. In the treatment of cancer, a sufficiently low temperature, termed "lethal temperature," should be ensured to achieve effective destruction of the target volume. Mazur [7] defined the lethal temperatures for cell destruction within the range of $-5\,^{\circ}\mathrm{C}$ to $-50\,^{\circ}\mathrm{C}$. Intracellular ice forms in prostate cells at temperatures below $-40\,^{\circ}\mathrm{C}$ [8], which, therefore, serves as a target temperature in this application. Other investigators suggest that even higher temperatures, e.g., $-20\,^{\circ}\mathrm{C}$, may be lethal to the cells [9].

The cooling rate maintained at the freezing front, has also been implicated as a key factor, which determines the probability of survival of the frozen tissues [10]. Accordingly, for each cell type, there exist certain ranges of cooling rates, which, when applied at the phase-transition region behind the freezing front, would increase the probability of either cell survival or cell destruction. Typical plots of measured cell survival versus cooling rates shown in Fig. 1 [11] resemble bell-shaped curves. This implies that optimal conditions for cell destruction may be achieved only at either low or high cooling rates. At low cooling rates, of a few degrees Centigrade per minute, extracellular ice crystals are formed first. This disrupts the osmotic balance between the intra- and the extracellular fluids causing osmotic drying of the cell and its eventual shrinkage. This process, termed the "solution effect," may render the cell nonviable leading to its death upon thawing. Sharp intracellular ice crystals are formed at high cooling rates of hundreds degrees Centigrade per minute. This process, termed the "mechanical effect," may cause cell membrane leakage and, consequently, compromise its integrity leading to cell death upon thawing. At intermediate cooling rates, however, the experimental data suggest high probabilities of cell survival, rather than cell destruction. These processes were reviewed by Gage and Baust [12] and more recently by Hoffman and Bischof [13]. Figure 2 demonstrates schematically the effects of various cooling rates on biological cell behavior during phase-change.

It follows from the above discussion that precise and detailed information of the temperature field, which develops during the tissue freezing process, is essential to the surgeon, both at the pretreatment design stage as well as during the application stage. Such information may be obtained by solving the dynamic heat transfer problem involved. The problem to be solved, referred to as the "Stefan" problem, is nonlinear mainly due to the removal of the heat of fusion, which is liberated at the moving front separating the frozen and nonfrozen phases. In biological tissues, unlike pure substances, e.g., pure water, phase-change transition occurs over a temperature range rather than at a single temperature, a factor which further complicates the analysis. An additionally, rather complex associated problem, is the "inverse-Stefan" problem in which a certain predetermined cooling rate is to be imposed and maintained at the freezing front.

Analytical solutions to the Stefan problem are few [14–16] as are those involving phase-change in biological tissue [17–19]. Consequently, investigators revert to employing numerical solution techniques, e.g., front tracking method [20] or the enthalpy method [21,22]. The application of multiprobes in tissuelike substances were analyzed by Keanini and Rubinsky [23] who presented a general technique for optimizing cryosurgical procedures. Rabin and Stahovich [24] and Rabin et al. [25] introduced cryoheaters as a means of controlling the extent of the multiprobes' frozen region in order to protect certain tissue regions from being affected during the cryosurgical process. No experimental data were presented in any of these latter studies.

Rewcastle et al. [26] analyzed the ice ball formation around a single cryoprobe using an axisymmetric, finite difference model. Model predictions were compared with measured data and were shown to conform to within $\pm 5\,^{\circ}\mathrm{C}$. Jankun et al. [27] developed an interactive software simulation package (CRYOSIM) for cryoablation of the prostate by liquid nitrogen-operated cryoprobes. The model is based on a finite difference numerical technique. Acquired ultrasound data were used to perform on-line adjust-

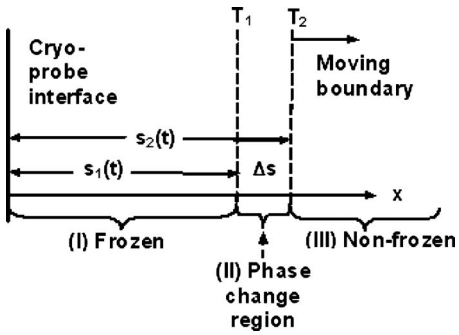

Fig. 3 Schematic representation of phase change in biological materials

ments of model parameters and in the prediction of the temporal variations of the isothermal surfaces in the prostate. The package facilitates the simulation and tracking of the "therapeutic temperature" in the prostate. Baissalov et al. discussed a semi-empirical treatment planning model for optimization of multiprobes [28]. A finite elements procedure was developed to analyze the 3D heat transfer problem in a model of the prostate. Predicted locations of the frozen front were compared with experimental X-ray readings to within ± 2 mm. The optimization procedure was demonstrated by simulating the placement of six cryoprobes at equal radial distances in a medium around a central urethral warmer. Rewcastle et al. [29] presented a 3D finite difference analysis of ice ball formation for one, three, and five cryoprobes. Results of the 3.4 mm OD diameter, high pressure Argon-operated probes with 30 mm long active segments, yielded good conformity to experimental data in gelatin. The authors defined an "ablation ratio" as the percentage volume of a certain temperature, which is considered ablative or lethal to the tissue, relative to the total frozen volume. The value of this ratio for their three-probe configuration was calculated at 0.21. Wan et al. [30] presented a finite element model of multiprobe cryosurgery of the prostate, which was based on a variational principle. Model results were verified by comparison to an analytical solution of an idealized problem and to experimental data obtained for a single probe. The case of six-probe symmetric positioning in the prostate was simulated and 2D quadrant results were demonstrated. The authors define a "freezing exposure index," which relates the combined effect of freezing temperature and the duration the tissue is held at this temperature, as an index of damage caused to the tissue.

This article presents a retrospective work performed at the Technion, Israel Institute of Technology, over the last 3-odd decades. Results of analytical and numerical solutions are presented briefly as well as experimental data and their comparison to the derived results. Studies include the analysis of both the direct (Stefan) and the inverse-Stefan phase-change heat transfer problems in a tissue-simulating medium (gel) by the application of both surface and insertion cryoprobes. The effects of blood perfusion and metabolic heat generation rates on the advancement of the freezing front are presented. The simultaneous operation of needle cryoprobes in a number of different configurations and the effects of a thermally significant blood vessel in the vicinity of the cryoprobe are also presented and discussed.

2 Formulation of the Phase-Change Problem

With reference to Fig. 3, and without loss of generality, the phase-change problem is presented as one-dimensional in Cartesian coordinates. The phase changing medium (PCM) is assumed to behave such as a "real" substance in which phase transition occurs over a range of temperatures, unlike "pure" substances, which are characterized by a single phase-transition temperature. Three stages are identified in the evolution of the freezing front in the PCM.

Stage 1: The PCM is initially at a certain spatially distributed temperature and remains completely nonfrozen (liquid stage) through the end of this stage. At the beginning of the cryosurgical procedure and thereafter, the temperature of the cryoprobe (heat sink) is being lowered according to a certain preplanned time-dependent trajectory, removing sensible heat from the medium. This stage ends when the cryoprobe-medium interface reaches T_2, which defines the upper temperature boundary of the phase-change region.

Stage 2: During this stage an intermediate phase (liquid +solid) begins to form and expands adjacent to the cryoprobe. Solid ice crystals co-exist with the yet nonfrozen surrounding medium. Sensible heat with gradually increasing portions of latent heat are removed from the PCM in this region. Only sensible heat is pumped out of the rest of the medium, which remains nonfrozen. This stage ends when the cryoprobe-medium interface reaches T_1, which defines the lower temperature boundary of the phase-change region below which the entire PCM is in the frozen state (solid).

Stage 3: In this stage three regions exist in the medium: (a) a completely frozen region (solid) adjacent to the cryoprobe, $0 > x > s_1(t)$, the upper temperature boundary of which is T_1, (b) an intermediate region $s_1(t) > x > s_2(t)$ in which phase transition occurs, bounded by T_1 and T_2, and (c) a yet nonfrozen region (liquid), the lower boundary of which is located at $x = s_2(t)$ and is bounded by T_2 and T_∞.

Similar to other problems involving heat transfer in biological entities, the heat balance of the phase-change problem is assumed to be governed by the bioheat equation [31], Eq. (1).

$$\rho c_p \frac{\partial T}{\partial t} = k \frac{\partial^2 T}{\partial x^2} + w_b c_b (T_a - T) + q_m \tag{1}$$

where ρ and ρ_b are the tissue and blood densities, kg/m^3, respectively, c_p and c_b are the tissue and blood specific heat capacities, J/kg K, respectively, T(x,t) is the tissue temperature, °C, x is the length coordinate, m, t is the time, s, k is the tissue thermal conductivity, W/m K, w_b is the capillary blood perfusion rate, kg_b/m^3 s, T_a is the blood temperature, °C, and q_m is the metabolic heat generation rate, W/m^3.

Equation (1) may be assumed to apply in tissue regions, wherein blood flow and metabolic heat generation persist. In the present case this equation applies in region III. In region I, upon completion of freezing, both capillary blood perfusion ($w_b = 0$) and metabolic heat generation ($q_m = 0$) cease and Eq. (1) reduces to the simple transient heat equation. Blood continues to flow in major blood vessels, at least for awhile, even under these conditions, and would require the formulation of an additional, coupled heat balance equation, as shown subsequently. In the phase-transition region II a gradual cessation of both capillary blood perfusion ($w_b \to 0$) and metabolic heat generation ($q_m \to 0$) are assumed.

The following general boundary and continuity conditions may be specified for this problem:

$$\text{at } x = 0 \text{ (cryoprobe-medium interface):} \quad T_I(x,0) = T_{pr}(t) \tag{2}$$

$$\text{at } x = s_1(t) \text{ (beginning of phase-change region):} \quad T_I = T_{II} = T_1 \tag{3a}$$

$$\text{and} \quad k_I \frac{\partial T_I}{\partial x} = k_{II} \frac{\partial T_{II}}{\partial x} \tag{3b}$$

$$\text{at } x = s_2(t) \text{ (end of phase-change region)} \quad T_{II} = T_{III} = T_2 \tag{4a}$$

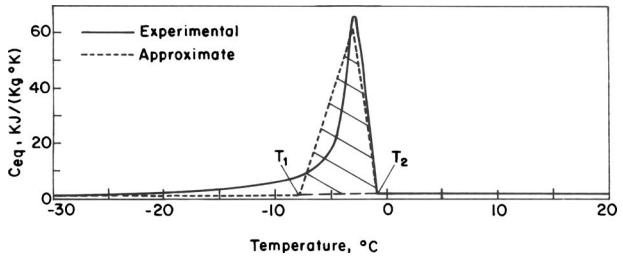

Fig. 4 Equivalent specific heat for "Tylose" (24% methylcellulose/76% water by mass) as a function of temperature in the phase-change region [32]. (Copyright 1974 by Elsevier. Reproduced with permission of Elsevier via Copyright Clearance Center.)

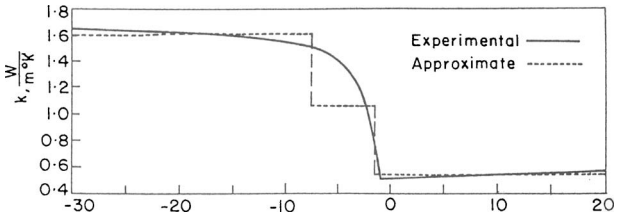

Fig. 5 Thermal conductivity of "Tylose" as a function of temperature in the phase-change region [32]. (Copyright 1974 by Elsevier. Reproduced with permission of Elsevier via Copyright Clearance Center.)

$$\text{and} \quad k_{II}\frac{\partial T_{II}}{\partial x} = k_{III}\frac{\partial T_{III}}{\partial x} \tag{4b}$$

In the intermediate region II, wherein the liquid and solid phases co-exist, accounting for the latent heat of freezing yields the following heat balance equation:

$$\rho c_{II}\frac{\partial T_{II}}{\partial t} = k_{II}\frac{\partial^2 T_{II}}{\partial x^2} + \rho L\frac{df_s}{dt} \tag{5}$$

where L is latent heat of freezing, J/kg, and f_s is the solid fraction in this region defined by Eq. (6).

$$f_s = \frac{1}{L}\int_{T_1}^{T_{II}} (c - c_{eq})dT \tag{6}$$

where c_{eq} is equivalent specific heat capacity, e.g., Fig. 4, which approximates the absorbed latent heat in this region, and

$$f_s = 0 \quad \text{for} \quad T_{II} = T_2 \tag{7a}$$

$$f_s = 1 \quad \text{for} \quad T_{II} = T_1 \tag{7b}$$

$$\text{at } x \to \infty \text{ (constant temperature):} \quad T(\infty,t) = T_\infty \tag{8}$$

At t=0 the initial temperature distribution of the tissue is given by

$$T(x,0) = T_{Init}(x) \tag{9}$$

3 Tissue Thermophysical and Physiological Properties

Tissue thermophysical properties assume different values in the nonfrozen and frozen regions. Table 1 lists plausible values for various tissue properties as applied in our studies. In the intermediate phase-transition region II, these properties vary appreciably with the temperature. Data in the literature present experimentally measured variations for latent heat and thermal conductivity of high water content materials, compare. Figs. 4 and 5 [32]. This behavior may be assumed as a first approximation of tissue behavior under similar conditions. Accounting for these changes in the analysis may be done by either following the measured changes precisely or approximately, as shown by the broken lines in Figs. 4 and 5.

Capillary blood perfusion and metabolic heat generation decrease from their normothermia values as the tissue temperature is lowered. As the upper temperature bound of the phase-transition range T_1 is reached, both these variables, may be assumed to decay to zero. Certain courses of change of these variables may be assumed, e.g., Ref. [33].

3.1 Solutions of the Phase-Change Problem. The phase-change problem may be characterized either as a regular Stefan or an inverse-Stefan problem. In the former the course of change of the temperature at the interface with the cryoprobe is assumed to be known. Accordingly, the temperature distribution in the freezing medium, the time-dependent location of the freezing front and the temperature rate of change at this front are to be determined. In the inverse-Stefan problem, on the other hand, a desired temperature rate of change is to be imposed at the freezing front. The purpose of the analysis is to determine the temperature changes (forcing function) that should be applied at the tissue-cryoprobe interface in order to satisfy this condition.

Due to the inherent nonlinearity of this class of problems, the analytical solutions are difficult to derive and are therefore rather limited. Numerical solution schemes have greatly expanded the computational capabilities and dominate this field of research. Below are presented a few of our analytical derivations and additional numerical treatments.

3.1.1 Analytical Solutions of the Stefan Problem in Biological Media. Rubinsky and Shitzer [17] presented an analytical solution in Cartesian coordinates of a Stefan-like problem in a biological tissue in contact with a cryoprobe. Equation (1) was solved subject to the assumption $T_2 \to T_1$, i.e., a single phase-transition temperature similar to pure substances. The effects of blood perfusion and of metabolic heat generation rates, on medium temperature variations, heat flux and frozen front location are shown in Figs. 6 and 7, respectively. Table 2 lists the parameters used in the computational cases. According to these figures, the heat flux in the medium increase as both w_b and q_m decrease. In general, varying

Table 1 Ranges of thermophysical and physiological property values

Property	Units	Range of values: Nonfrozen	Range of values: Frozen	References
Specific heat capacity of tissue	kJ/kg K	3.52–4.1	1.84–1.9	17, 34, and 36
Specific heat capacity of blood	kJ/kg K	3.64	(-)	[15]
Thermal conductivity	W/m K	0.385–0.63	1.3–2.25	17, 34, 36, 38, and 39
Density	kg/m^3	1000	1000	[34]
Latent heat of freezing	kJ/kg	233–330		17, 34, and 38
Phase change temperature	°C	−1 to −2	−7 to −8	17, 34, 37, and 39
Capillary blood perfusion rate	kg/m^3 s	0–10	(-)	[17]
Metabolic heat generation rate	kW/m^3	0–251	(-)	[17]

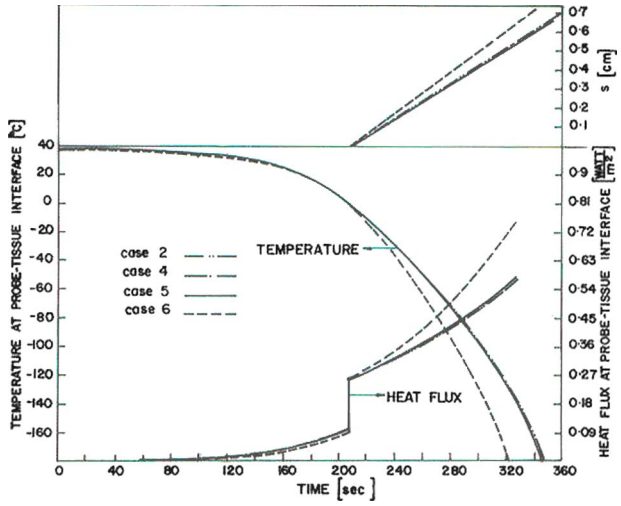

Fig. 6 Cryoprobe temperature and heat flux variations and frozen front location versus blood perfusion rates [17]

the metabolic rate in the yet nonfrozen tissue will have minor effects on all the plotted variables, except when it reduces to zero.

Table 2 Combinations of physiological parameters used in the computations [17]

Case	1	2	3	4	5	6
q_m, kW/m^3	251	251	251	167	84	0
w_b, kg/m^3 s	10	7.0	4.0	7.0	7.0	0
$T_{arterial}$, °C	37.7	38	38.7	37.6	37.3	37

Blood perfusion, on the other hand, does affect the course of change of the plotted variables as it changes, hindering, as is to be expected, the advancement of the frozen front.

Budman et al. provided a combined analytical and integral solution around an embedded general purpose cryoprobe [34]. The liquid nitrogen-operated probe was tested experimentally in pure water with a 2% gelatin agar. Results were compared with the analytical predictions and are shown in Fig. 8.

3.1.2 Analytical Solutions of the Inverse-Stefan Problem in Biological Media. Rabin and Shitzer [19] extended the analysis of the inverse-Stefan problem to a freezing biological medium. The tissue model, assumed initially at a uniform temperature, was depicted by a semi-infinite, thermally homogeneous, and isotropic medium. The problem was analyzed by the "enthalpy method" [35] with the latent heat of freezing expressed by the variable

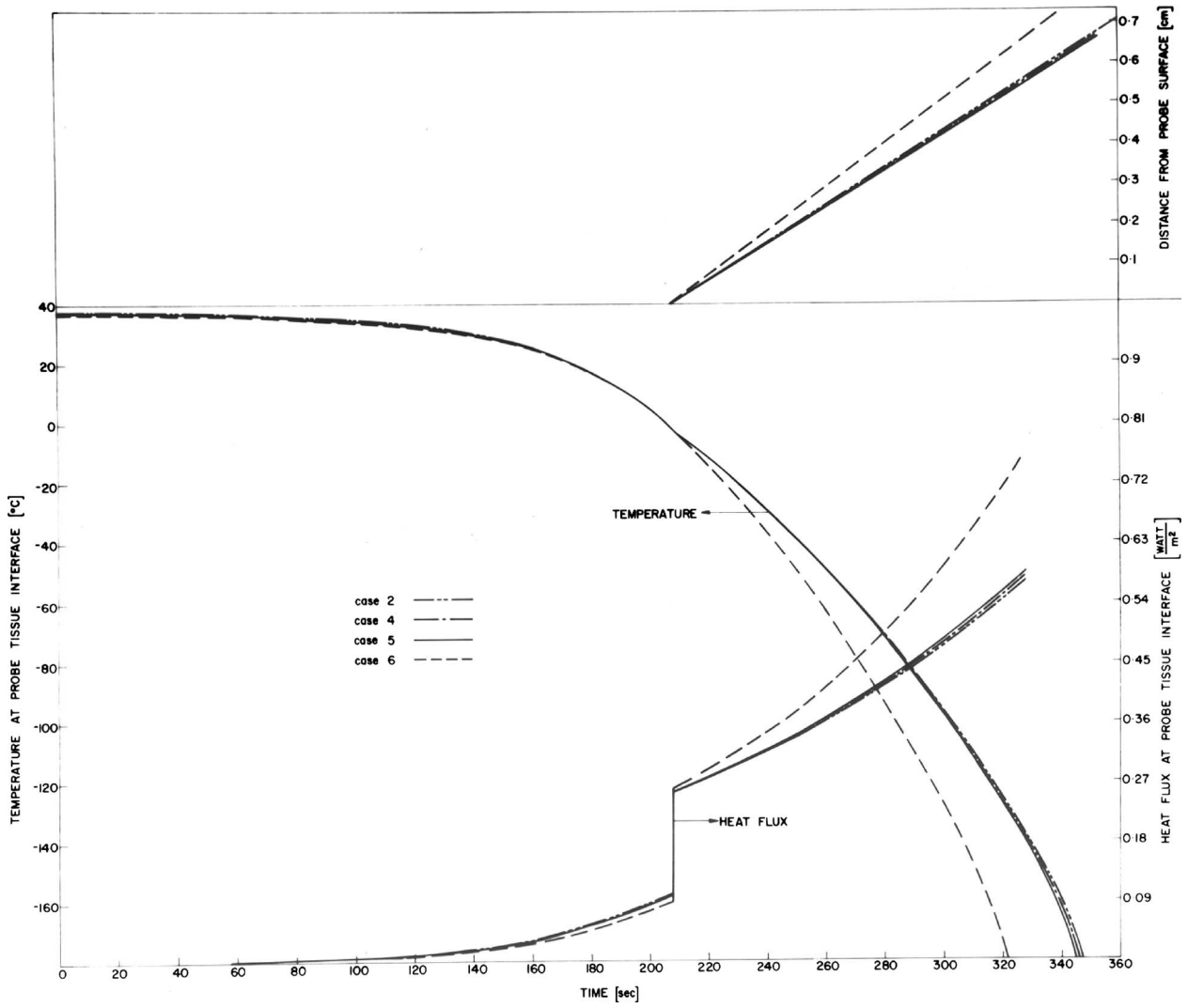

Fig. 7 Cryoprobe temperature and heat flux variations and frozen front location versus metabolic heat rates [17]

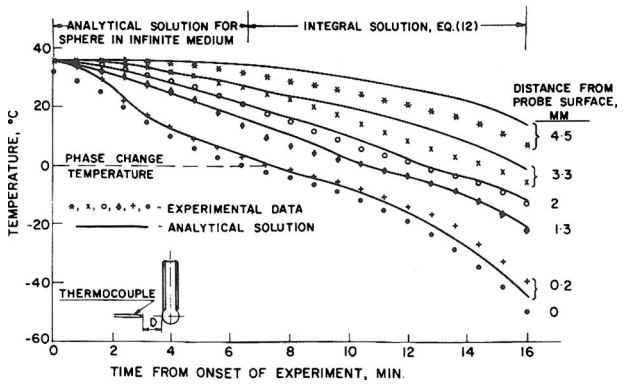

Fig. 8 Comparison of experimental and analytical temperature distributions around a general purpose cryoprobe [34]

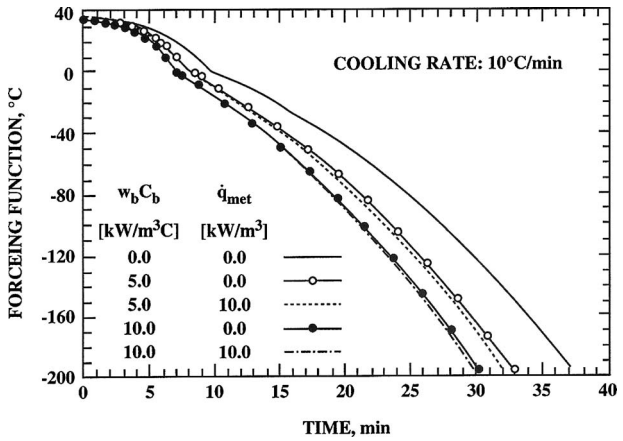

Fig. 9 Forcing functions of the inverse-Stefan problem for various combinations of heat sources and a cooling rate of 10°C/min at the frozen front [19]

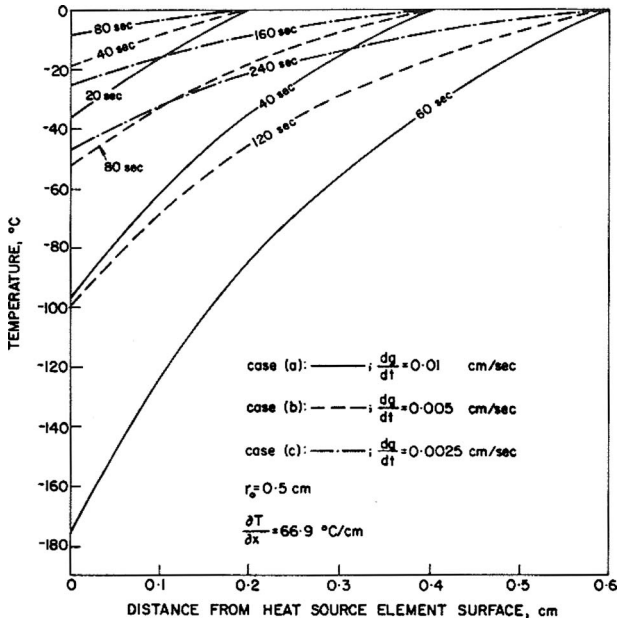

Fig. 10 Temperature distributions in a PCM for a constant heat flux and various velocities of the moving boundary. Spherical geometry [36].

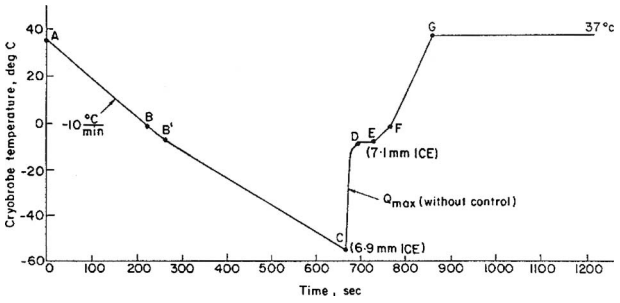

Fig. 11 Calculated forcing function for the controlled freezing/thawing processes for a maximal cooling/warming rate of 10°C/min [37]

volumetric specific heat. Results compared very well to the analytic solution presented by Rubinsky and Shitzer [36] by setting the phase-transition temperature range to $T_1-T_2=0.1°C$, closely approximating an ideal PCM. Assuming a cooling rate of 10°C/min, the calculated forcing function at the cryoprobe-medium interface is plotted in Fig. 9 as a function of capillary blood perfusion and metabolic heat generation rates. It is observed that blood perfusion has a much more profound effect than does metabolic heat generation. When comparing the behavior of the forcing function to the case of a nonbiological medium ($w_b \rightarrow 0$ and $q_m \rightarrow 0$), maximally assumed blood perfusion and metabolic heat generation rates reduce the duration of the cryotreatment by about 20%, the depth of freezing by about 15% and the phase-transition width by about 37%.

3.1.3 Analytical Solutions of the Inverse-Stefan Problem in Nonbiological Media. The inverse-Stefan problem in a nonbiological medium ($w_b \rightarrow 0$ and $q_m \rightarrow 0$) was solved analytically by Rubinsky and Shitzer [36] in Cartesian and spherical coordinates. Assuming a single phase-change temperature and a known temperature gradient at the moving freezing front, a series solution was derived for the temperature distribution in the medium. This solution facilitates the calculation of the temperature variations required at the cryoprobe-medium interface (forcing function) so as to achieve the desired thermal conditions at the moving front. Figure 10 presents temperature distributions in a PCM, depicted by spherical geometry, for a constant heat flux at and various velocities of the moving boundary. It is seen that the higher the velocity of the freezing front, the steeper are the temperature gradients in the medium. This demands lower temperatures to be

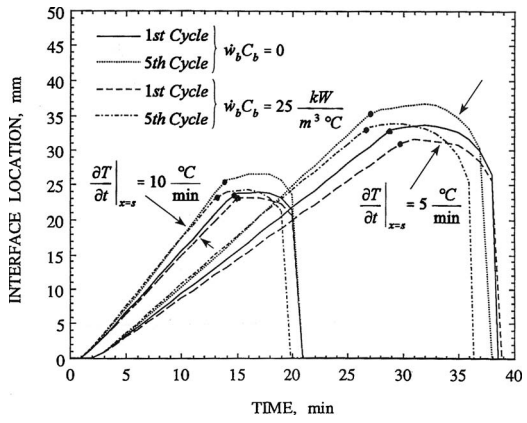

Fig. 12 Freezing front locations, for the first and fifth repeated freezing/thawing cycles, for various blood perfusion rates and cooling/warming rates. The dots indicate end of cooling and initiation of warming in each cycle [40].

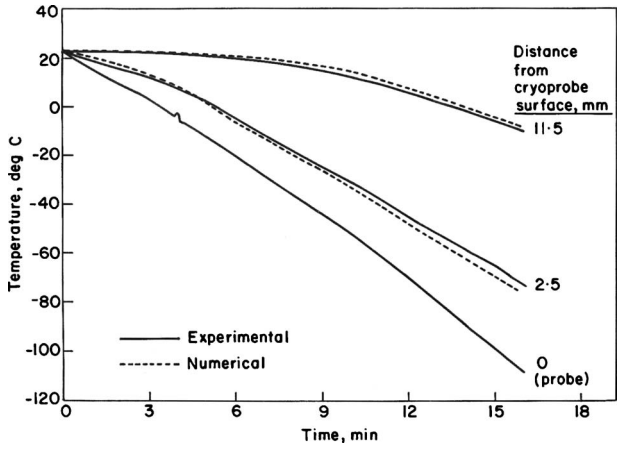

Fig. 13 Comparison of experimental and computational finite element results [39]

imposed at the cryoprobe-medium interface and may, therefore, limit the extent of freezing, should the required front velocity be excessively high.

An integral solution of a one-dimensional inverse-Stefan problem was presented by Budman et al. [37]. They assumed phase change to occur over a range of temperatures and analyzed both the controlled freezing and the subsequent thawing processes of the PCM. A constant cooling rate, $\partial T/\partial t = H$, was imposed at the lower phase-transition temperature T_1. Medium thermophysical properties were those shown in Table 1 and Figs. 4 and 5. Figure 11 shows the variations of the calculated forcing function during a single freeze-thaw cycle for uniform cooling/heating rates of $\pm 10°C/min$. Control characteristics of the cryosurgical process in a nonideal medium simulating a biological tissue were determined by Budman et al. [38]. Using a proportional-integral controller, the stability of the process was analyzed. It was shown that the desired cooling rate at the phase-change front deviated from the desired value only by about 1%.

Rabin and Shitzer [33] solved the inverse-Stefan problem of a biological tissue undergoing repeated freezing/thawing cycles. The locations of the freezing front following the first and fifth cycles are plotted in Fig. 12. Data are shown for two cooling/warming rates of $5°C/min$ and $10°C/min$ and for two cases of capillary blood perfusion: $w_bC_b = 25\ kW/m^3°C$ and for no blood perfusion. It is seen that the freezing front velocity is almost linearly dependent on time during the freezing stage, for all cases shown. The location of the freezing front seems to be only weakly dependent on blood perfusion during the first cycle. It does penetrate deeper during the initial portion of the thawing stage, in the case of no blood perfusion due to thermal inertia. In all cases studied, the maximal depth of freezing during the fifth cycle was about 7% larger than in the first cycle.

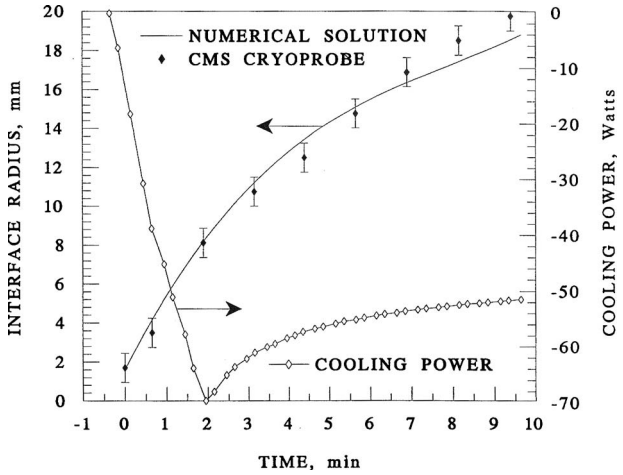

Fig. 14 Comparison of measured [41] and calculated freezing front location around a 3.4 mm cylindrical Accuprobe. Required cooling power was estimated by the numerical code [40].

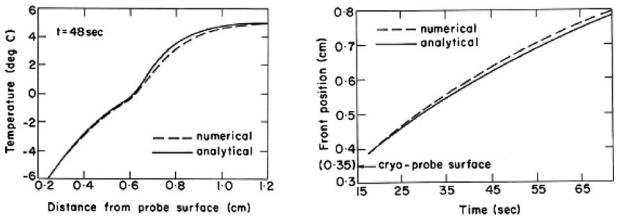

Fig. 15 Comparison of numerical and analytical temperature distributions (left) and freezing front location (right) for a single, infinitely long cryoprobe embedded in a PCM [21]

3.1.4 Numerical Solutions of the Inverse-Stefan Problem in Biological Media. Budman et al. [39] performed a numerical analysis of the freezing process in a nonideal medium. A new cryosurgical device was developed, which facilitated the achievement of a specified cooling rate at the phase-change front by accurately controlling probe temperature variations. An electrical heating element was wrapped around the shaft of the cryoprobe as a means to control its temperature by off-setting the excessive heat extraction of the cryogen. The system was tested in an aqueous-mashed potatoes solution. A closed loop control system was used with the cryoprobe surface temperature as the feedback variable. The energy balance equations were solved by a finite elements scheme and showed good conformity to measured results, Fig. 13. The tracking accuracy of the desired temperature trajectory of the cryoprobe was to within $\pm 4°C$. Supercooling of the PCM and liquid nitrogen boiling instabilities were identified as the main reasons for deviations from the set-point.

An axisymmetric finite difference solution of the inverse-Stefan problem in a PCM simulating a biological tissue was presented by Rabin and Shitzer [40]. The cylindrical probe, with a finite active length, was assumed to be embedded in an infinite PCM. The solution was verified both against an analytical derivation of a simpler case and experimental data [41], showing good conformity. A parametric study included the cooling power of the cryoprobe and the dimensions of the frozen region, Fig. 14. For a 3.4 mm o.d. probe and 10 min of operation, the required heat extraction power increased gradually for the first 2 min of operation, reaching a maximum of about 70 W. Thereafter, as the heat load on the probe decreased with the thickening of the frozen phase, which acted as a thermal insulator, the cooling power decreased slowly to about 50 W.

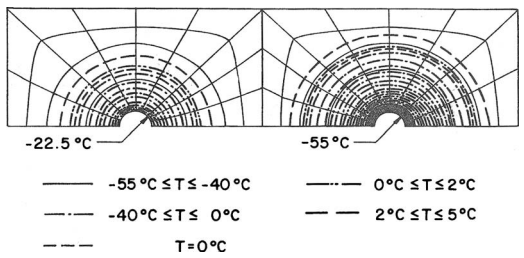

Fig. 16 Temperature distributions after 60 s for nonsymmetrical activation of two adjacent cryoprobes at –55°C/1°C/s (right) and –22.5°C/0.5°C/s (left) [21]

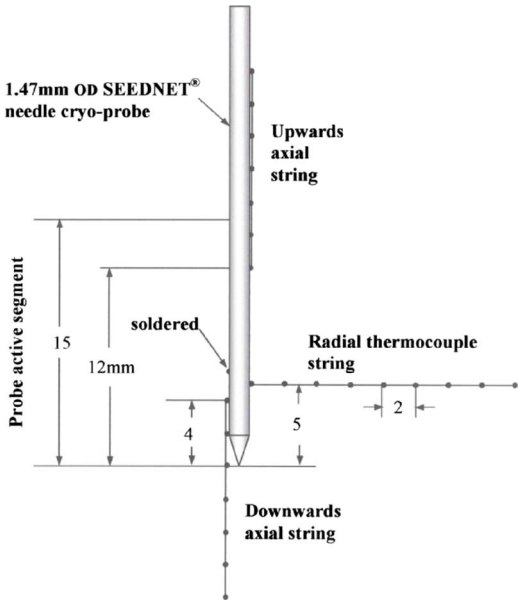

Fig. 17 Placement of the thermocouple junctions adjacent to the insertion cryoprobe. Dimensions in millimeter [44].

3.1.5 Numerical Analyses of the Stefan Problem for Multiprobe Insertion in a PCM. Finite element analysis of the temperature field around two adjacent cryoprobes was presented by Weill et al. [21]. The infinitely long cylindrical probes were assumed to be embedded in an infinite medium, initially at a constant temperature (5°C). For simplicity the medium was assumed to be homogeneous and isotropic and the effects of both metabolic heat generation and capillary blood perfusion were neglected. In order to test the solution of the developed numerical scheme, the calculated results of a single embedded probe were compared with available analytical results, Fig. 15. The performance of two embedded cryoprobes was calculated for both symmetrical and nonsymmetrical operations. In the symmetrical mode, the surface temperatures of both probes was dropped abruptly and maintained thereafter at this level. Calculated isotherms around each probe were circular during the first minute of operation and became skewed afterwards, "bulging" at the sections away from the centerline separating the probes [21]. The nonsymmetrical operation

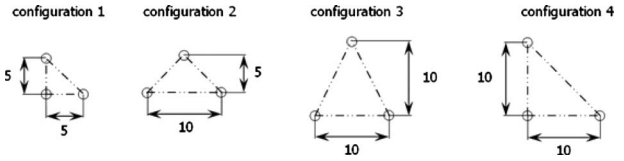

Fig. 19 Insertion configurations for three cryoneedles [43]. Dimensions in mm. (Copyright 2007 by Elsevier. Reproduced with permission of Elsevier via Copyright Clearance Center.)

involved simultaneously dropping of one probe to −55°C while the other was dropped to only −22.5°C. In addition, cooling rates applied were 1°C/min and 0.5°C/min, respectively. Temperature distributions around both probes are shown in Fig. 16. As is to be expected, the temperature field generated by the higher temperature probe lags considerably behind that produced by the lower temperature probe.

Magalov et al. [42–44] applied ANSYS 7.0 to analyze the thermal behavior of one, two, and three insertion needle cryoprobes operated by high pressure Argon gas. A single and two SEEDNET® cryoneedles, placed at varying distances apart, were tested in Agar gel the temperatures of which were monitored radially and axially, as shown in Fig. 17 [44]. Figure 18 compares measured and computed isothermal contours of 0°C, −20°C, and −40°C for a single probe after 6 min and 10 min, and 0°C and −40°C isotherms for two probes, 10 mm apart, after 10 min of operation. The synergistic effects of three cryoneedles were studied numerically. All probes were operated uniformly and were placed at the apexes of four triangles, as determined by the 5 × 5 mm placement template used in this industry [45], Fig. 19. Figure 20 shows the locations of the 0°C, −20°C, and −40°C isotherms for all placement configurations after 1 min and 10 min of operation. For all cases studied the volumes enclosed by the lethal isotherm (assumed here as −40°C), achieve most of their size in the first minutes of operation thus obviating the need for prolonged applications [43]. Furthermore, it was demonstrated that percentage volumes occupied by this lethal isotherm, relative to the total frozen volume, after 10 min of operation, will be only about 6% (single probe), 6–11% (two probes, varying distances apart) and 6–15% (three probes, different placement configurations) [43].

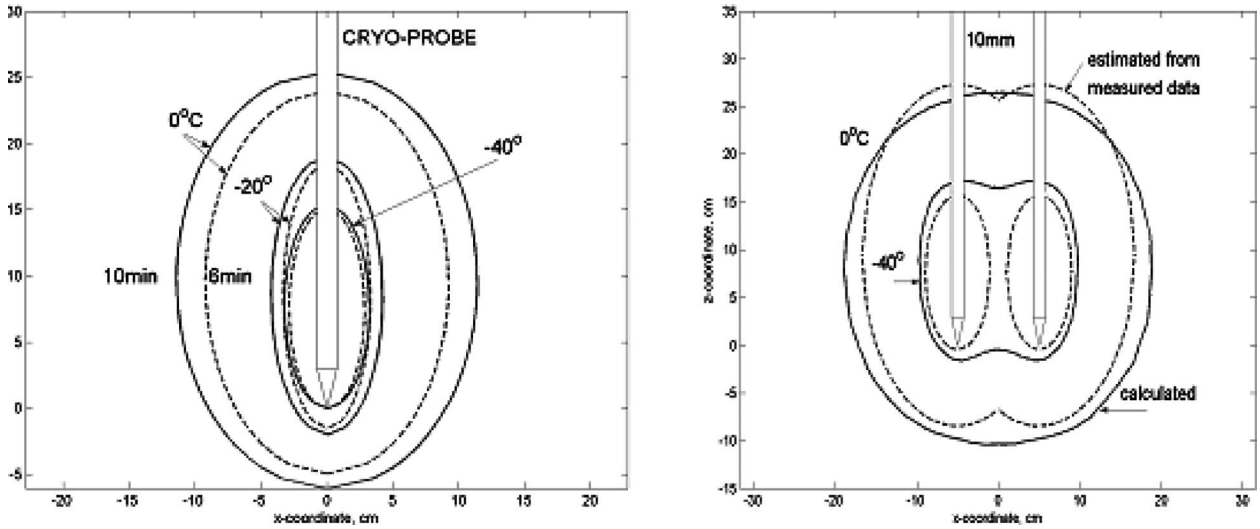

Fig. 18 Measured and estimated isothermal contours for one (left) and two 10 mm apart (right) cryoprobes after 10 min of operation [44]

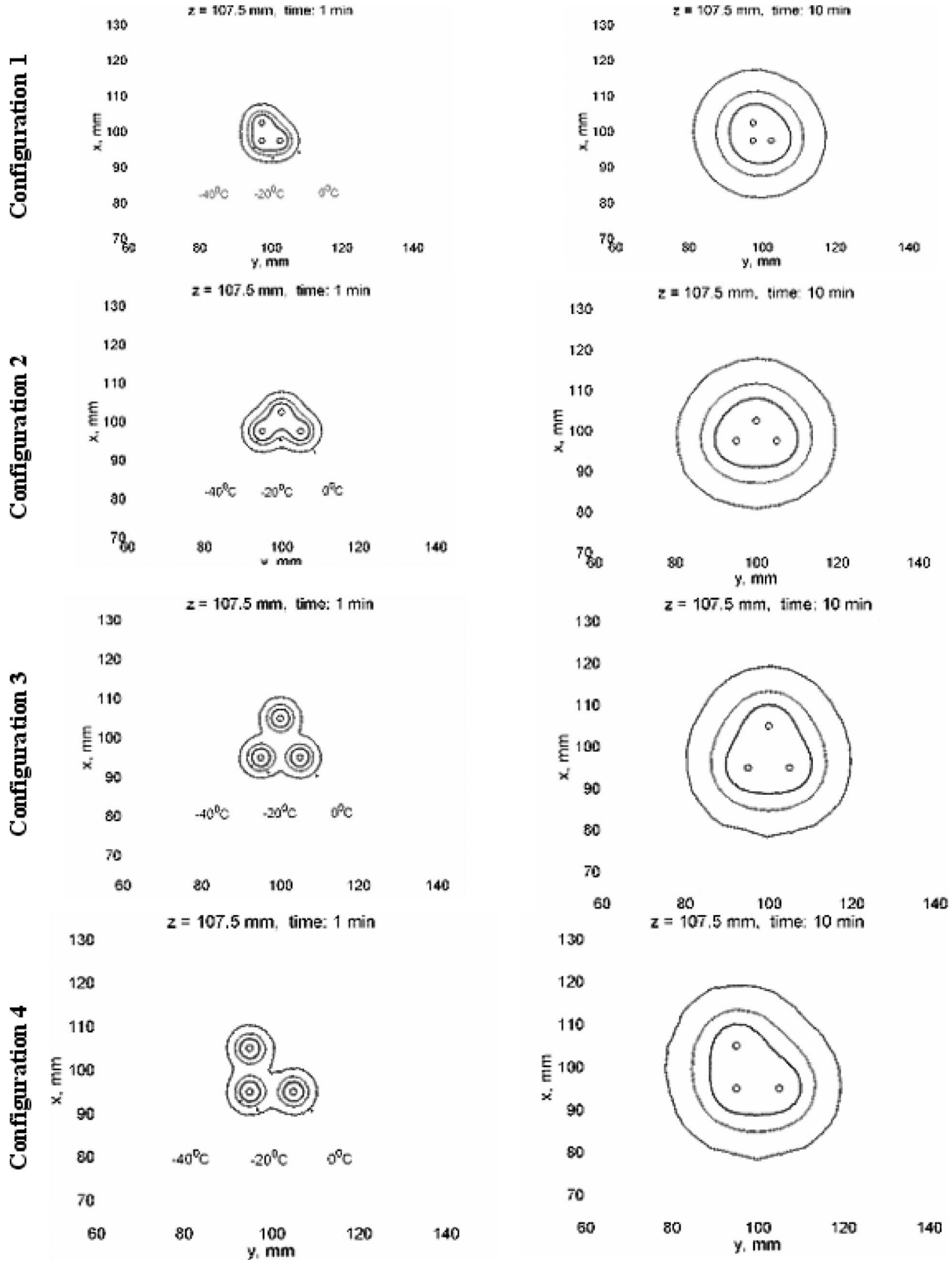

Fig. 20 Top views of 0°C, −20°C, and −40°C isothermal contours for different placement configurations after 1 min and 10 min of operation of three cryoneedles [43]. (Copyright 2007 by Elsevier. Reproduced with permission of Elsevier via Copyright Clearance Center.)

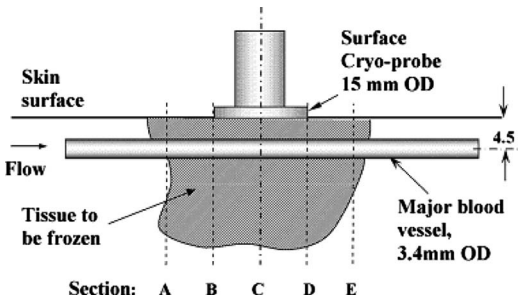

Fig. 21 Schematic view of the tumor, embedded blood vessel, and surface cryoprobe [48]

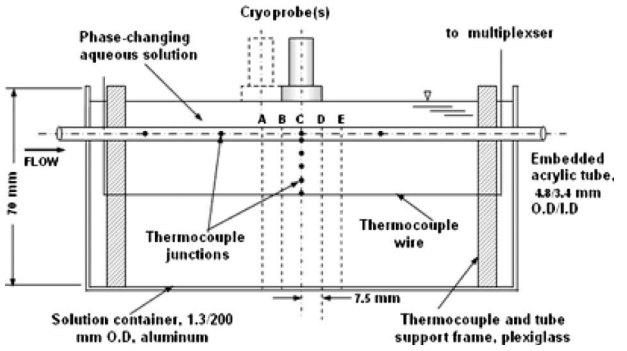

Fig. 22 Cross-sectional view of the test section holding the embedded tube and thermocouples in the PCM [47]

3.1.6 Effects of an Embedded Thermally Significant Blood Vessel. The effects of an embedded, thermally significant, blood vessel on the temperature field in a tissue-simulating PCM subjected to freezing by a surface cryoprobe were studied experimentally [46–48] and numerically [49]. The surface cryoprobe was operated by liquid nitrogen and was placed flush with the surface of the PCM, Fig. 21 [48]. A tube simulating a blood vessel was embedded in the PCM parallel and close to the surface, coincident with the cryoprobe centerline, Fig. 22 [47]. The tube was perfused by warm water at a constant temperature. Computer connected thermocouples were arranged on a single plane inside the PCM and were spaced sparingly, utilizing the symmetry of the setup to minimize thermal perturbations by the thermocouple wires. Each experiment involved five repetitions with the probe placed alternately at each one of the sections A–E, Fig. 22.

Variations of the isothermal surfaces in the PCM were interpolated from the recorded temperatures. A numerical solution of the phase-change problem under these conditions was developed using ANSYS 7.0. The numerical code was adapted to include the thermal interaction between the PCM and the water perfused em-

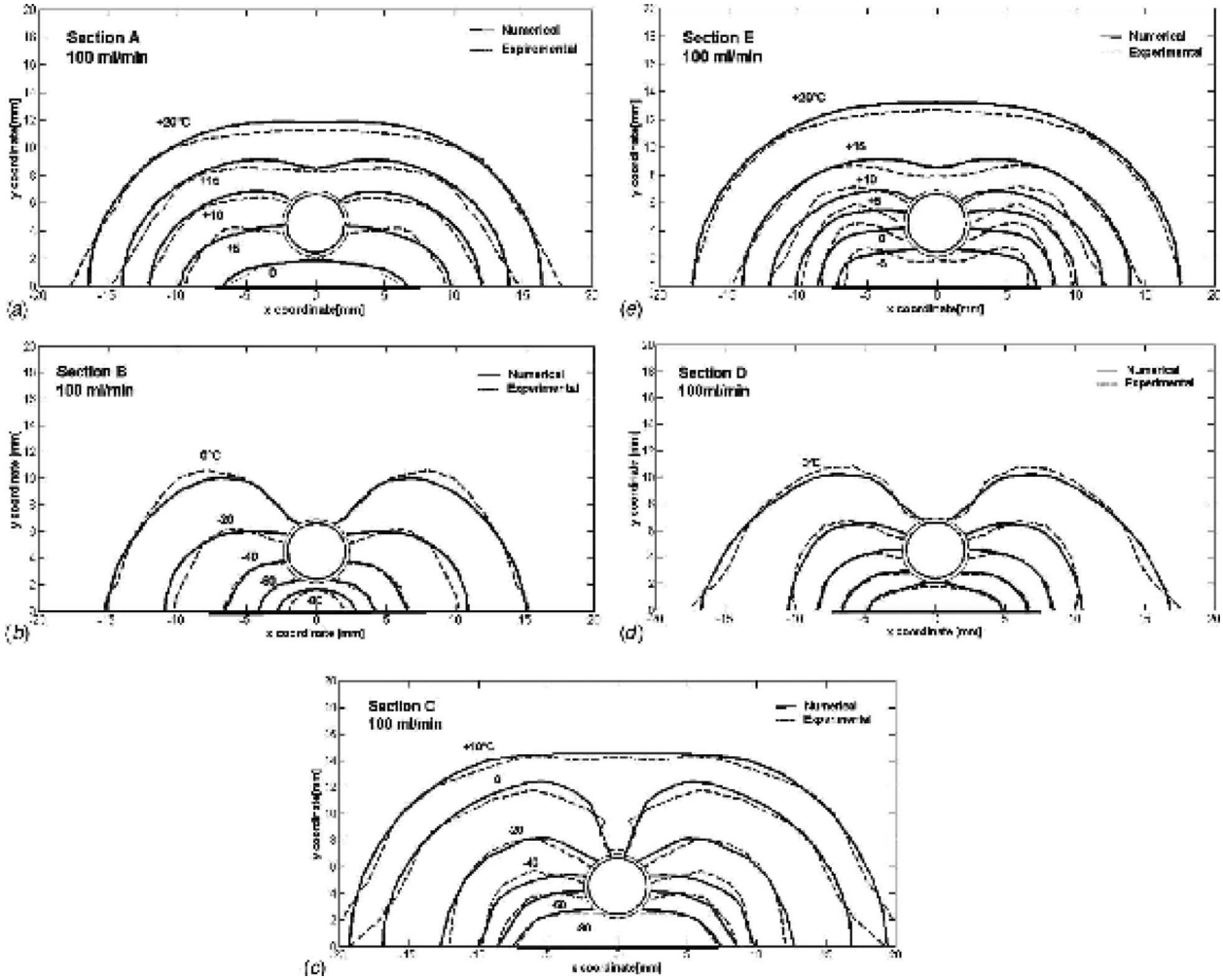

Fig. 23 Measured and computed isotherms in sections A–E in the PCM after 20 min of cryoprobe operation at –8°C/min. Embedded tube flow rate: 100 ml/min [49].

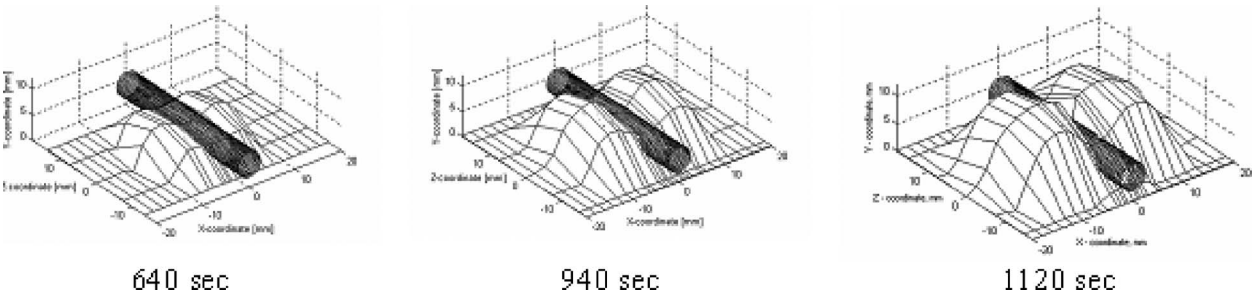

Fig. 24 Three-dimensional snap shots of the progression of the 0°C isothermal surface in the vicinity of the embedded tube [47]. Cryoprobe operates from underneath.

bedded tube [49]. Figure 23 compares the measured and computed isothermal contours in the PCM after 20 min of operation of the cryoprobe and 100 ml/min flow rate in the tube. Figure 24 depicts 3D approximations of the frozen front in the PCM at three instances, clearly showing the gradual engulfing of the embedded tube by the PCM [47].

3.2 In Vivo Experiments. Based on the previous work of Budman et al. [39], Rabin and Shitzer [50], and Rabin et al. [51] developed a new cryosurgical device, which was tested in vivo on the skeletal muscle of a rabbit's hind leg. Cryoprobe-medium interface temperature was controlled to follow the desired trajectory by activating an electrical heater wrapped around the cryoprobe shaft. Figure 25 shows the histological appearance of muscle cells 7 days post-cryotreatment. A gradual interface, of about 0.5 mm thickness, is observed between the cryo-injured tissue and the adjacent noninjured cells. The difference between the two regions is quite pronounced manifesting the potency of the cryotreatment.

4 Conclusion

The studies cited in this article summarize work done in our laboratory of Heat Transfer in Biological Systems for the last 3-odd decades. These studies address a variety of issues relating to the analysis of heat exchange driven by cryoprobes during the phase-change process in biological and nonbiological media alike. The studies included the development of both analytical solutions, wherever applicable, and numerical solution schemes, which, recently, rely for the most part on available commercial codes. In certain cases experimental studies, conducted both in vivo and in vitro, complemented the analyses.

For cryosurgery to become the treatment-of-choice, much more work will be required, among other things to cover the following issues:

1. a clear cut understanding and definition of the tissue-specific conditions that are required to ensure the complete destruction of a tissue undergoing a controlled cryosurgical process. The current conflict and resulting ambiguity between specifying either a tissue-specific lethal temperature or, conversely, a desired cooling rate at the freezing front, hinder progress in this inherently complex subject.
2. more comprehensive analyses, which address, in addition to the freezing stage, the more involved controlled thawing stage and its consequences on the overall outcome of the complete freeze/thaw cycle(s).
3. improved technical means to control the temperature variations of the cryoprobe to achieve the desired thermal conditions required for tissue destruction.
4. improvement in the pretreatment design process to include optimal placement schemes of multiprobes and their separate and specific operation.
5. understanding the effects of thermally significant blood vessels, and other related thermal perturbations, which are situated adjacent to, or even within, the tissue to be destroyed.

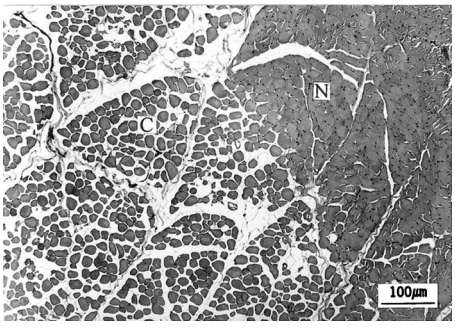

Fig. 25 Low power magnification of the interface between normal (N) and cryodamaged fibers (C) 7 days post-cryotreatment [51]. Copyright 1996 by Elsevier. Reproduced with permission of Elsevier via Copyright Clearance Center.

Acknowledgment

The studies presented in this retrospective article are the results of concerted efforts by many individuals, most of whom were graduate students under the author's guidance at the Technion. They are listed here in chronological order: Boris Rubinsky, Hector Budman, Anne Weill, Yoed Rabin, Yehoshua Chayut, Loay Massalha, Zaur Magalov, Genady Beckerman, and Noga Rybko. Colleagues of mine have also contributed in their specialized fields: Stefano Del Giudice, Yehoshua Dayan, Pinhas Bar-Yoseph, Raymond Coleman, Rosalie Ber, Daniel Mordohovich, and David Degani. Dr. Nir Berzak conducted experiments with the SEEDNET® cryoprobe. The cryosurgical equipment in our laboratory was purchased by a generous grant from the Caesaria Foundation, Israel. The James H. Belfer Chair in Mechanical Engineering provided financial support throughout the years.

I am forever indebted and grateful to all those individuals and organizations for their participation, support, and contributions.

References

[1] Onik, G., 1996, "Cryosurgery," Crit. Rev. Oncol. Hematol., **23**, pp. 1–24.
[2] Rubinsky, B., and Onik, G., 1991, "Cryosurgery: Advances in the Application of Low Temperatures to Medicine," Int. J. Refrig., **14**, pp. 190–199.
[3] Shepherd, J., and Dawber, R. P. R., 1982, "The Historical and Scientific Basis of Cryosurgery," Clin. Exp. Dermatol., **7**, pp. 321–328.
[4] Gage, A. A., and Huben, R. P., 2000, "Cryosurgical Ablation of the Prostate," Semin. Urol. Oncol., **5**, pp. 11–19.
[5] Zouboulis, C. C., 1998, "Cryosurgery in Dermatology," Eur. J. Dermatol., **8**, pp. 466–474.
[6] http://en.wikipedia.org/wiki/Cryopreservation
[7] Mazur, P., 1968, "Physical-Chemical Factors Underlying Cell Injury in Cryosurgical Freezing," *Cryosurgery*, R. Rand, A. Rinfret, and H. von Leden, eds., Thomas, Springfield, IL, pp. 32–51.
[8] Saliken, J. C., Donnelly, B. J., and Rewcastle, J. C., 2002, "The Evolution and State of Modern Technology for Prostate Cryosurgery," Urology, **60**, pp. 26–33.
[9] Zisman, A., Pantuck, A. J., Cohen, J. K., and Belldegrun, A. S., 2001, "Prostate Cryoablation Using Direct Transperineal Placement of Ultrathin Probes Through a 17-Gauge Brachytherapy Template—Technique and Preliminary

Results," Urology, **58**, pp. 988–993.
[10] Orpwood, R. D., 1981, "Biophysical and Engineering Aspects of Cryosurgery," Phys. Med. Biol., **26**, pp. 555–575.
[11] Crister, J. K., and Morbaaten, L. E., 2000, "Cryopreservation of Murine Spermatozoa," Institute for Laboratory Animal Research, J. Cryobiology of Embryos, Germ Cells & Ovaries, **41**(1), pp. 197–206.
[12] Gage, A., and Baust, J., 1998, "Mechanisms of Tissue Injury in Cryosurgery," Cryobiology, **37**, pp. 171–186.
[13] Hoffmann, N. E., and Bischof, J. C., 2002, "The Cryobiology of Cryosurgical Injury," Urology, **60**, pp. 40–49.
[14] Stefan, J., 1891, "Uber die Theorie des Eisbildung, insbesondere uber die Eisbildung im Polarmeere," Ann. Phys. Chem., **42**(2), pp. 269–286.
[15] Neumann, F., 1912, "Lectures Given in the 1860's," *Die Partielen Differentialglechungen der Mathematischen Physik*, 5th ed., B Riemann and H. Weber, eds., Vieweg und Sohn, Braunschweig, Vol. 2, pp. 117–121.
[16] Ozisik, M. N., and Uzzell, J. C., 1979, "Exact Solution for Freezing in Cylindrical Symmetry With Extended Freezing Temperature Range," ASME J. Heat Transfer, **101**, pp. 331–334.
[17] Rubinsky, B., and Shitzer, A., 1976, "Analysis of a Stefan-Like Problem in a Biological Tissue Around a Cryosurgical Probe," ASME J. Heat Transfer, **38**, pp. 514–519.
[18] Trezek, G. J., 1985, "Thermal Analysis for Cryosurgery," *Heat Transfer in Medicine and Biology: Analysis and Applications*, A. Shitzer and R. C. Eberhart, eds., Plenum, New York, pp. 239–259.
[19] Rabin, Y., and Shitzer, A., 1995, "Exact Solution for the Inverse Stefan Problem in Non-Ideal Biological Tissues," ASME J. Heat Transfer, **117**, pp. 425–431.
[20] Shamsundar, N., and Sparrow, E. M., 1975, "Analysis of Multidimensional Conduction Phase Change Problem via the Enthalpy Method," ASME J. Heat Transfer, **97**, pp. 333–340.
[21] Weill, A., Shitzer, A., and Bar-Yoseph, P., 1993, "Finite Elements Analysis of the Temperature Field Around Two Adjacent Cryo-Probes," ASME J. Biomech. Eng., **115**, pp. 374–379.
[22] Dalhuijsen, A. J., and Segal, A., 1986, "Comparison of Finite Element Techniques for Solidification Problems," Int. J. Numer. Methods Eng., **23**, pp. 1807–1829.
[23] Keanini, R. G., and Rubinsky, B., 1992, "Optimization of Multiprobe Cryosurgery," ASME J. Heat Transfer, **114**, pp. 796–801.
[24] Rabin, Y., and Stahovich, T. F., 2003, "Cryoheater as a Means of Cryosurgery Control," Phys. Med. Biol., **48**, pp. 619–632.
[25] Rabin, Y., Lung, D. C., and Stahovich, T. F., 2004, "Computerized Planning of Cryosurgery Using Cryoprobes and Cryocatheters," Technol. Cancer Res. Treat., **3**(3), pp. 229–243.
[26] Rewcastle, J. C., Sandison, G. A., Hahn, L. J., Saliken, J. C., McKinnon, J. G., and Donnelley, B. J., 1998, "A Model for the Time-Dependent Thermal Distribution Within an Iceball Surrounding a Cryoprobe," Phys. Med. Biol., **43**, pp. 3519–3534.
[27] Jankun, M., Kelly, T. J., Zaim, A., Young, K., Keck, R. W., Selman, S. H., and Jankun, J., 1999, "Computer Model for Cryosurgery of the Prostate," Comput. Aided Surg., **4**, pp. 193–199.
[28] Baissalov, R., Sandison, G. A., Donnelley, B. J., Saliken, J. C., McKinnon, J. G., Muldrew, K., and Rewcastle, J. C., 2000, "A Semi-Empirical Planning Model for Optimization of Multiprobe Cryosurgery," Phys. Med. Biol., **45**, pp. 1085–1098.
[29] Rewcastle, J. C., Sandison, G. A., Muldrew, K., Saliken, J. C., and Donnelley, B. J., 2001, "A Model for the Time Dependent Three-Dimensional Thermal Distribution Within Iceballs Surrounding Multiple Cryoprobes," Med. Phys., **28**(6), pp. 1125–1137.
[30] Wan, R., Liu, Z., Muldrew, K., and Rewcastle, J. C., 2003, "A Finite Element Model for Ice Ball Evolution in a Multi-Probe Cryosurgery," Comput. Methods Biomech. Biomed. Eng., **6**(3), pp. 197–208.
[31] Pennes, H. H., 1948, "Analysis of Tissue and Arterial Blood Temperature in the Resting Human Forearm," J. Appl. Physiol., **1**, pp. 93–122.
[32] Bonacina, C., Comini, G., Fasano, A., and Primicerio, M., 1974, "On the Estimation of Thermophysical Properties in Nonlinear Heat Conduction Problems," Int. J. Heat Mass Transfer, **17**, pp. 861–867.
[33] Rabin, Y., and Shitzer, A., 1997, "Combined Solution of the Inverse Stefan Problem for Successive Freezing/Thawing in Nonideal Biological Tissues," ASME J. Biomech. Eng., **119**(2), pp. 146–152.
[34] Budman, H., Shitzer, A., and Del Giudice, S., 1986, "Investigation of Temperature Fields Around Embedded Cryoprobes," ASME J. Biomech. Eng., **108**(1), pp. 42–48.
[35] Goodman, T. R., 1958, "The Heat Balance Integral and Its Application to Problems Involving a Change of Phase," Trans. ASME, **80**, pp. 335–342.
[36] Rubinsky, B., and Shitzer, A., 1978, "Analytic Solutions to the Heat Equation Involving a Moving Boundary With Application to the Change of Phase Problem (The Inverse Stefan Problem)," ASME J. Heat Transfer, **100**, pp. 300–303.
[37] Budman, H., Shitzer, A., and Dayan, Y., 1995, "Analysis of the Inverse-Stefan Problem of Freezing and Thawing of a Binary Solution During Cryosurgical Processes," ASME J. Biomech. Eng., **117**(2), pp. 193–202.
[38] Budman, H., Dayan, J., and Shitzer, A., 1991, "Control of the Cryosurgical Process in Non-Ideal Materials," IEEE Trans. Biomed. Eng., **38**(11), pp. 1141–1153.
[39] Budman, H., Dayan, J., and Shitzer, A., 1991, "Controlled Freezing of Non-Ideal Solutions With Applications to Cryosurgical Processes," ASME J. Biomech. Eng., **113**(4), pp. 430–437.
[40] Rabin, Y., and Shitzer, A., 1998, "Numerical Solution of the Multidimensional Freezing Problem During Cryosurgery," ASME J. Biomech. Eng., **120**, pp. 32–37.
[41] Chang, Z., Finkelstein, J. J., and Baust, J., 1994, "Development of a High-Performance Multiprobe Cryosurgical Device," Biomed. Instrum. Technol., **42**, pp. 383–390.
[42] Magalov, Z., Shitzer, A., and Degani, D., 2006, "Simulation of Cryo-Ablation of the Prostate by 1, 2 and 3 Embedded Cryo-Surgical Probes," Proceedings of the 13th International Heat Transfer Conference, Vol. BHT-04, pp. 1–12.
[43] Magalov, Z., Shitzer, A., and Degani, D., 2007, "Isothermal Volume Contours Generated in a Freezing Gel by Embedded Cryo-Needles With Applications to Cryo-Surgery," Cryobiology, **55**(2), pp. 127–137.
[44] Magalov, Z., Shitzer, A. and Degani, D., 2008, "Experimental and Numerical Study of 1, 2 and 3 Embedded Needle Cryo-Probes Simultaneously Operated by High Pressure Argon Gas," ASME J. Heat Transfer, **130**(3), p. 032301.
[45] Galil-Medical, Ltd., Yokneam, Israel, 2003, Experimental Data, private communication.
[46] Chayut, Y., and Shitzer, A., 1996, "Simulating the Effects of a Large Blood Vessel on the Temperature Field around a Surface Cryoprobe," ASME Advances in Heat and Mass Transfer in Biotechnology, L. J. Hayes and S. Clegg, eds., ASME, New York, pp. 21–22.
[47] Massalha, L., and Shitzer, A., 2004, "Freezing by a Flat, Circular Surface Cryoprobe of a Tissue Phantom With an Embedded Cylindrical Heat Source Simulating a Blood Vessel," ASME J. Biomech. Eng., **126**(6), pp. 736–744.
[48] Rybko, N., Shitzer, A., and Degani, D., 2009, "Experimental simulation of a Thermally Significant Blood Vessel in a Tissue Subjected to Cryo-Surgery," Proceedings of the Seventh World Conference on Experimental Heat Transfer, Fluid Flow and Thermodynamics, Krakow, Poland, pp. 193–200.
[49] Beckerman, G., Shitzer, A., and Degani, D., 2009, "Numerical Model of the Effects of a Thermally-Significant Blood Vessel on Solidification by a Circular Surface Cryosurgical Probe Compared to Experimental Data," ASME J. Heat Transfer, **131**(5), p. 051101.
[50] Rabin, Y., and Shitzer, A., 1996, "A New Cryosurgical Device for Controlled Freezing. Part 1: Setup and Validation Tests," Cryobiology, **33**, pp. 82–92.
[51] Rabin, Y., Coleman, R., Mordohovich, D., Ber, R., and Shitzer, A., 1996, "A New Cryosurgical Device for Controlled Freezing. Part 2: In Vivo Experiments on Skeletal Muscle of Rabbit Hindlimbs," Cryobiology, **33**, pp. 93–105.